

Final version published in *Analytical Chemistry*, 2017, 89 (17), pp 8908–8916.

<https://pubs.acs.org/doi/abs/10.1021/acs.analchem.7b01379>

Revised Manuscript: July 16, 2017

Integrated smartphone-app-chip system for on-site ppb-level colorimetric quantitation of aflatoxins

Xiaochun Li,^{†,*} Fan Yang,[†] Jessica X. H. Wong,[‡] and Hua-Zhong Yu^{†,‡,*}

[†]Key Laboratory of Advanced Transducers and Intelligent Control Systems (Ministry of Education and Shanxi Province), College of Physics and Optoelectronics, Taiyuan University of Technology, Shanxi 030024, P.R. China

[‡]Department of Chemistry, Simon Fraser University, Burnaby, British Columbia V5A 1S6, Canada

* Corresponding authors. lixiaochun@tyut.edu.cn (X.L.); hogan_yu@sfu.ca (H.Y.)

Abstract: We demonstrate herein an integrated, smartphone-app-chip (SPAC) system for on-site quantitation of food toxins, as demonstrated with aflatoxin B1 (AFB1), at parts-per-billion (ppb) level in food products. The detection is based on an indirect competitive immunoassay fabricated on a transparent plastic chip with the assistance of a microfluidic channel plate. A 3D-printed optical accessory attached to a smartphone is adapted to align the assay chip and to provide uniform illumination for imaging, with which high-quality images of the assay chip are captured by the smartphone camera and directly processed using a custom-developed Android app. The performance of this smartphone-based detection system was tested using both spiked and moldy corn samples; consistent results with conventional ELISA kits were obtained. The achieved detection limit (3 ± 1 $\mu\text{g}/\text{kg}$, equivalent to ppb) and dynamic response range (0.5–250 $\mu\text{g}/\text{kg}$) meet the requested testing standards set by authorities worldwide. We envision that the integrated SPAC system promises to be a simple and accurate method of food toxin quantitation, bringing much benefit for rapid on-site screening.

Keywords: aflatoxins; smartphone; mobile app; microchip; on-site chemical analysis, colorimetric quantitation

Introduction

Aflatoxins are a class of toxic and carcinogenic molecules produced by certain molds (*Aspergillus flavus* and *Aspergillus parasiticus*), which are regularly found in improperly stored food products (e.g. chili peppers, corn, peanuts, rice, and wheat). As they are harmful to the health of humans and animals, serious food safety problems have occurred all over the world as a result of aflatoxin contamination of cereals and feedstuffs.¹ Beginning in 2002, these food toxins have been listed as Group 1 carcinogens by the International Agency for Research on Cancer;² to date at least 14 aflatoxins have been identified with aflatoxin B1 (AFB1), B2 (AFB2), G1 (AFG1) and G2 (AFG2) as the major species of concern. In particular, AFB1 possesses the highest toxicity and carcinogenicity; long-term exposure to low concentrations of AFB1 can lead to adverse immuno-competence effects, growth, and disease resistance, while a single, high level exposure can cause acute hepatitis and hemorrhagic necrosis in humans and animals.^{1,3} It is with this concern that most countries have established exposure limits for AFB1; in China and the US, the maximum permissible level of AFB1 is 20 µg/kg (ppb) in corns and groundnuts.^{4,5}

In order to detect and quantitate AFB1 in food products, a variety of analytical methods have been established. The conventional approaches include high performance liquid chromatography (HPLC),⁶ liquid chromatography-mass spectrometry (LC-MS),⁷ and enzyme-linked immunosorbent assay (ELISA).^{8,9} These techniques have high test accuracy and sensitivity but are time-consuming and require trained professionals to operate specialized instrumentation. For on-site screening of AFB1, gold immunochromatography assay (e.g., rapid test strips) offers a low-cost, rapid and simple detection protocol.¹⁰ Nevertheless, these rapid test strip scan only provide qualitative or semi-quantitative results; a simple and portable method for quantitative determination of AFB1 is highly desired to fulfill the needs of food safety supervision.

Spectrophotometer-like optical readers have been adapted for many years as portable detectors in fluorescence-based assays (e.g., using quantum dots or nanosilica particles) for a range of analytes that include proteins, drugs, and toxins.¹¹⁻¹³ In more recent years, technology is evolved such that

smartphones have been adapted as a newer generation of detection tools due to their powerful imaging capabilities and the open source app development environment.¹⁴⁻²¹ Smartphone-based analytical techniques have also attracted increasing attention for health-related and food safety monitoring. For example, Coskun et al. built a food allergen testing platform with a specially designed optical attachment to image and analyze immunoassays performed in micro-wells; the smartphone camera was used to acquire transmission images of the assay.²² Yu et al. developed a disposable lateral flow-through strip to examine the alkaline phosphatase activity in raw milk;²³ in this case, the smartphone camera was used to monitor the color change induced by the accumulation of gold nanoparticles. Lee et al. recently demonstrated a one-dot lateral flow immunoassay (LFIA) for AFB1 by using a smartphone in conjunction with a LFIA reader.²⁴

In this work, we demonstrate an integrated smartphone-app-chip (SPAC) system for the quantitation of AFB1 at parts-per-billion (ppb) level (equivalent to $\mu\text{g}/\text{kg}$) in corn samples; the improvement of the detection limit was based on the silver-enhanced indirect competitive immunoassay fabricated on a transparent plastic chip and the quantitative colorimetric analysis with a custom designed Android app. We also utilized a cost-effective optical attachment, readily fabricated with a 3D printer, to provide uniform illumination for imaging the plastic chip and to improve the accuracy of the grayscale reading. The research stems from, but is not limited to the above mentioned pioneering adaptation of smartphone and accessories as powerful analytical devices,¹⁴⁻²⁴

Experimental Section

Reagents and Materials

Aflatoxin B1-bovine serum albumin (AFB1-BSA) conjugate, mouse monoclonal anti-AFB1 antibody, AFB1 standard, Tween 20, gelatin, citric acid, N-hydroxysuccinimide (NHS) and N-(3-Dimethylaminopropyl)-N'-ethylcarbodiimide hydrochloride (EDC) were purchased from Sigma-Aldrich (St. Louis, USA). Bovine serum albumin (BSA), sodium chloride (NaCl), sodium dihydrogen phosphate (NaH_2PO_4), disodium hydrogen phosphate (Na_2HPO_4) were purchased from Aladdin (Shanghai, China). Nanogold (1.4 nm diameter)-streptavidin conjugate was ordered from

Nanoprobes Inc. (New York, USA) and biotin labeling kit-NH₂ from Dojindo Laboratories (Kumamoto, Japan). Trisodium citrate, hydroquinone, and silver nitrate were from Kermel (Tianjin, China). Sylgard 184 silicone elastomer kit was purchased from Dow Corning (Midland, MI, USA). Transparent polycarbonate (PC) sheet of 1.0 mm thickness was purchased from Bayer (Leverkusen, Germany). The commercial AFB1 ELISA kit was purchased from Wise Science & Technology Development Co., Ltd. (Zhenjiang, China).

Fabrication of the optical attachment for smartphone imaging

As shown in Figure 1a, the main component of the optical attachment consists of a special light source and a chip slot (holding the plastic assay chip in place) that allows the test chip to be directly imaged with a smartphone (Huawei Honor 3C, 8MP Camera with F/2.0 aperture and 28 mm focal length lens, shown in Figure 1b). The frame of the attachment was designed in Autodesk (Inventor) and fabricated with a 3D printer (Qingxin-M8). As depicted in the right inset of Figure 1a, 16 white light-emitting diodes (LEDs, 2 × 3 × 4 mm) were assembled at the edges of a light guide plate (LGP, 51 × 51 × 4 mm, Cathyly), which was placed below a reflector (51 × 51 × 1 mm, Cathyly) and above a diffuser (53 × 53 × 1.5 mm, Cathyly). The LGP is made of polymethyl methacrylate (PMMA), with a designed pattern of scattering dots printed on the top side. The top part of the attachment is a battery compartment (with a switch) holding two AAA batteries (1.5 V), which provide the power for the LED lights. Figure 1b shows how a plastic assay chip is imaged with the optical attachment on a smartphone. In this case, the attachment is upside down, which makes the image acquisition and subsequent analysis convenient for the user.

Android app for smartphone-based chip imaging and analysis

A custom-designed app, named AFB1DET, for imaging and analyzing the assay chips was compiled using the Android Developer Tools in Java. It was installed and tested on a smartphone running Android 4.4.2. Aside from the chip imaging, data analysis can be performed with the same app, i.e., a captured image will be processed directly and the test results are displayed on the smartphone screen. The overall work-flow of this “AFB1DET” app can be described as follows (Figure 2):

- (a) The “AFB1DET” app starts to run on the smartphone after the user clicks on the AFB1DET icon. The main interface displays three options for the user to select: New Test, History, and Instructions (Figure 2a).
- (b) When a new test is chosen, the rear camera of the smartphone is powered on and a preview with a red box is displayed on the screen. It has been designed to display eleven red bars for the signals and three blue bars for the background, all within the red box that the user aligns with the assay strip. When the user selects the “Capture” function, the camera obtains an image of the region of interest (ROI) of the assay chip. The image is subsequently converted into a grayscale image and stored in the smartphone’s internal memory.
- (c) To obtain quantitative information on the test, the user can select the “Analyze” option; the captured image is then analyzed by the app and the test results, i.e., the calculated concentrations of AFB1 in the unknown samples are displayed on the screen immediately (Figure 2c).

Images captured by the phone’s camera are typically displayed in the RGB (red, green, blue) color space; however, the grayscale mode is required to quantitate the signal according to the luminosity value (grayscale intensity). The app has therefore been written to convert each pixel, from RGB to grayscale according to the general expression for the conversion of RGB pixel intensities into a grayscale intensity,²⁵

$$I = 0.30R + 0.59G + 0.11B \quad (1)$$

where R (red), G (green), B (blue) are the pixel intensities in their respective color channels and I is the grayscale intensity. We have adapted the optical darkness ratio (ODR) as the quantitation measure for analyzing the signal intensity of each strip, which is given by,²⁶

$$\text{ODR} = (I_b - I_s) / I_b \quad (2)$$

where I_b is the grayscale value of the background and I_s the grayscale value of the test strip. Here, we define the strips as the test regions made by the PDMS channel plate and the background as the region between the channels. A rectangular region (9×260 pixels) around the strip is used to calculate the averaged gray scale value of each strip and three rectangular regions (23×260 pixels) between strips are used to calculate the averaged gray value of the background. The ODR of each

strip is obtained by equation 2. The calibration equation and its correlation coefficient are calculated with the method of least squares according to the concentrations of AFB1 standard solutions and the corresponding ODR values. On the basis of the calibration equation and the obtained ODR values, we subsequently determined the concentrations of AFB1 in various samples (as described below).

Surface activation of the plastic chip and assay preparation

The PC sheets were first cleaned with ethanol and then treated in a UV/ozone cleaner (PSD-UV, Novascan Technologies Inc., Ames, USA) for 30 min to produce a hydrophilic surface with a high density of carboxylic acid groups.²⁷ The chip was subsequently immersed in a 0.1 M phosphate buffer at pH 6.0 containing 5.0 mM EDC and 0.3 mM NHS for 5 h to activate the surface carboxylic acid groups, followed by rinsing with deionized water and drying under a stream of N₂.

A PDMS (polydimethylsiloxane) plate (48 mm × 50 mm × 1 mm) with 11 embedded microchannels (0.5 mm × 25 mm × 50 μm) was placed directly on the surface of activated PC sheet (55 mm × 65 mm × 1 mm) and they were sealed together to prevent solution leakage by pressing the PDMS plate to the PC sheet firmly (Figure 3). Two holes punched into the PDMS on the ends of each channel as the inlet and outlet ports; the solution was injected into the inlet port using a micropipette and drawn through the channel by capillary action to the outlet port. Solution was removed with the aid of suction (e.g., using a micropipette) from the outlet port. To create the assay, a solution containing the AFB1-BSA conjugate (400 μg/mL) in 20 mM phosphate buffer (pH 7.4, 150 mM NaCl) was injected into each channel, and kept overnight at room temperature. The surface of each channel was then passivated by treating with 4% BSA in 20 mM phosphate buffer (pH 7.4, 150 mM NaCl) for 3 h.

For the sample testing, a mixture of 1 μL of biotinylated anti-AFB1 antibody (22 μg/mL) with either 1 μL of AFB1 standard solution (concentration ranging from 0-500 ng/mL) for the standards or 1 μL of the unknown corn samples (prepared as outlined below) was individually and sequentially injected into each channel and incubated for 30 min. The channels were rinsed with 20 mM phosphate buffer before nanogold-streptavidin conjugate solution in 20 mM phosphate buffer (pH 7.4, 150 mM NaCl,

0.1% BSA, and 0.05% NaN₃) was injected into the channels and incubated for 25 min. The PDMS plate was then removed and the plastic assay chip was thoroughly washed with deionized water, dried under N₂; it was subsequently immersed in a freshly made silver staining solution (48 mM silver nitrate and 192 mM hydroquinone) for 5 min to amplify the signals. At the end, the chip was thoroughly washed with deionized water to stop the reaction; it was dried under N₂ prior to imaging.

Real-world sample preparation and validation tests with ELISA and HPLC

In addition to testing standard solutions of AFB1, spiked fresh and moldy corn samples were also tested; the latter was obtained by incubating fresh corn in a humid environment at room temperature for one week to promote mold growth. In both cases, the corn samples were ground into fine powder (mortar and pestle). Extraction of aflatoxins was accomplished with methanol-water (7:3, v/v) containing 4% NaCl and vigorous shaking for 2 min. For spiked samples (0, 5, 10, 25 ng/mL), AFB1 standard was added to the mixture, stirred for 2 min and allowed to dry overnight before 0.5 mL of methanol-water was used to re-suspend the mixture.²⁸ The samples were then centrifuged for 5 min at 877 g (3500 rpm on a ZONKIA centrifuge HC-2518); aliquots of the supernatant were diluted by half with deionized water for samples that were to be tested with the SPAC system or ELISA.²⁹ The extracts to be tested with HPLC were filtered following centrifugation; the sample was first filtered with WhatmanTM Grade 4 filter paper, diluted with equal-amount of deionized water, then through a glass microfiber filter, and further extracted with an ISOLUTE Multimode SPE column at a flow rate of 6 mL/min. The column was washed with 20 mL (2 × 10 mL) water and then dried with air. AFB1 were eluted by passing 1 mL of methanol through the column at a flow rate of 1-2 mL/min. The eluate was evaporated to dryness at 45 °C under N₂ stream and the residue was re-dissolved with 1 mL of LC mobile phase solution (for HPLC tests).

To verify the accuracy of the developed SPAC system, a commercial AFB1 ELISA kit was used according to the manufacturer's instructions for the comparative study. Briefly, the different concentrations of AFB1 or spiked corn samples (50 µL/well), anti-AFB1 antibody, and anti-rabbit-HRP were sequentially added to the well and incubated for 30 min each at room

temperature. The ELISA plate was washed 4 times, and 100 μ L of TMB solution was added to each well and incubated for 15 min at 25 $^{\circ}$ C before adding the stop solution (2 M H_2SO_4 , 50 μ L/well). The absorbance at 450 nm was measured with a MultiskanTM GO Microplate Spectrophotometer (Thermo Fisher Scientific, Waltham, USA).

A Shimadzu HPLC system (LC-20AD, Tokyo, Japan) with a fluorescence detector was used to analyze both standard and corn samples. Chromatographic separations were performed on a reversed phase Shim-pack FC-ODS analytical column (75 \times 4.6 mm). Injection volumes of 10 μ L and the column temperature were maintained at 40 $^{\circ}$ C. The mobile phase was a solution of water-methanol (55+45), and the flow rate was 0.8 mL/min. To enhance the fluorescent responses of AFB1, an online and post-column derivatization was carried out with 0.05% of iodine solution at 0.2 mL/min in the CRB-6A of the HPLC system. The fluorescence detector was set to an excitation and emission wavelengths of 360 and 440 nm, respectively. The run time for one cycle was 10 min, and the retention times of AFB1 under these conditions were approximately 6.9 min.

Results and discussion

Chip-based competitive assay design and optimization

An indirect, competitive immunoassay for the detection of AFB1 (Figure 3) was conducted on a transparent plastic plate using pre-immobilized AFB1-bovine serum albumin (BSA) conjugates to capture labeled antibody in the presence of the target (free AFB1). As illustrated in Figure 3, the probe molecules, AFB1-BSA conjugates, were arrayed on the surface of the PC chip through surface coupling with the aid of a microfluidic channel plate. Upon introduction of a mixture containing the sample and biotinylated anti-AFB1 antibody, a competitive recognition reaction between the free AFB1 (in the sample) and the immobilized probe (AFB1-BSA conjugates) with the antibody occurs; free antibodies and those bound with free AFB1 were washed away. Nanogold-streptavidin conjugates added subsequently bind to biotinylated antibodies due to the strong biotin-streptavidin interaction. The assay signals are then amplified and visualized via the silver enhancement reaction;³⁰ because the amount of the surface-confined antibodies is inversely proportional to the

concentration of AFB1 in the sample, the grayscale intensities of thus formed binding strips correlate with the AFB1 concentration. Silver staining is required in order to enhance the signal as the gold nanoparticle conjugated to the streptavidin, at 1.4 nm in size, cannot be detected optically in the visible range. In amplifying the signal using the nanoparticle as a seed, the binding sites can be easily observed and quantitated with a flatbed scanner or a camera based on its optical darkness ratio.²⁷

For indirect competitive assays, both the amount of surface bound probes and the concentration of labeled antibodies subsequently added influence the detection sensitivity and dynamic response range. Therefore, we have carried out systematic tests to optimize the assay conditions (Figure 4). To confirm the optimal concentration of AFB1-BSA conjugates to be immobilized, different concentrations repeated in triplicates over two orders of magnitude (from 25 to 1000 $\mu\text{g/mL}$) of AFB1-BSA were tested while maintaining the concentration of biotinylated antibodies in solution (22 $\mu\text{g/mL}$; no free AFB1 present). The optical image of the chip in Figure 4a, obtained using a flatbed scanner in grayscale mode, clearly shows the increased darkness of the strips as the concentration of AFB1-BSA gradually increased. The grayscale intensity was analyzed using the histogram tool in Adobe Photoshop and the ODR was calculated according to Equation 2. In Figure 4a, we plotted the ODR as a function of the concentration of AFB1-BSA; the ODR value initially increases with increasing concentration of AFB1-BSA (up to 400 $\mu\text{g/mL}$) and then reaches saturation. At this point, the highest surface coverage of AFB1-BSA conjugate should be achieved, and therefore, 400 $\mu\text{g/mL}$ of the AFB1-BSA probe was chosen for further experiments.

The optimal concentration of biotinylated anti-AFB1 antibody was then determined by testing a large range of concentrations (0.9-56 $\mu\text{g/mL}$), after the initial immobilization of AFB1-BSA (400 $\mu\text{g/mL}$). As shown in Figure 4b, the optical image of the chip shows that the darkness of the strips proportionally increased as the concentration of biotinylated anti-AFB1 antibody increased to 22 $\mu\text{g/mL}$. Above this concentration, further increase in the assay signal was not observed. It should be noted that the optimized conditions for the indirect competitive assay for AFB1 are restricted to the choice of substrate materials as well as the choice of particular monoclonal antibodies. In

comparison with standard ELISA reported previously that uses an enzyme-conjugated antibody,^{8,9} the signal amplification here relies on the gold nanoparticle promoted silver deposition at the assays sites.^{30,31} Nonetheless, the results shown in Figure 4 confirm that the competitive assay construction in conjunction with the silver staining signal amplification provides a colorimetric means for the quantitation of AFB1 (and other food toxins of interests).

Smartphone-app-chip system for AFB1 quantitation

For accurate quantitative colorimetric detection, a high quality image with accurate color/grayscale information is required. The lighting condition is one of the key factors that affect the quality of images taken by a smartphone.³² While scanners, as a professional image acquisition tool, can obtain high quality images with controlled lighting for film, photo, drawing,³³ they are not as portable or readily available as smartphones. As mentioned above, we designed and fabricated an optical attachment to control lighting by providing uniform illumination for smartphone imaging of the plastic assay chip. To evaluate the quality of images taken, particularly to ensure the effectiveness of the smartphone-app-chip integration, a series of ink bars with different, preset grayscale intensities ranging from 0 to 255 (top of Figure 5a) were printed on a plastic transparency sheet using an inkjet printer. The images obtained on a conventional office scanner and a smartphone (with the optical attachment) are shown in Figure 5a for a direct comparison. In both cases, the images are of high quality as the bars with different preset darkness values are differentiated well. The image captured with the smartphone appears to have a slightly darker, yet uniform background.

From the correlation plot of the ODR values obtained in two different ways (based on the images shown in Figure 5a), it was observed that the smartphone with the optical attachment provides comparable readings for the ink bars with low ODR values, i.e., deviations are observed for the darker bars on the right side (ODR > 0.6). In the linear range, the ODR values determined by the smartphone-app system demonstrates a great consistency with the ODR values obtained with a scanner with an $R^2 = 0.996$ (the slope is 1.02), confirming the accuracy of the SPAC system for a quantitative colorimetric/scannometric assay. With this experiment, it was determined that the simple,

3D-printed optical attachment is effective for obtaining high-quality image, which enables the adaptation of the integrated smartphone-app-chip system for real-world applications (i.e., quantitation of food toxins as described below).

With our integrated SPAC detection platform, a calibration curve can be created for every test to account for variations in assay environment and conditions. With the aid of a PDMS plate with 11 microchannels, as shown in Figure 6a, we were able to test 7 standard solutions, a blank, and three “unknown” samples at the same time. The “blank”, highlighted in a dashed red box, is an assay strip without the immobilization of AFB1-BSA conjugates, but all other reagents (biotinylated antibody, nanogold-streptavidin, and silver staining solutions) were added accordingly. From the low signal produced, it is clear that the non-specific adsorption of the antibodies on the chip surface is negligible. In contrast, with increased concentration of AFB1 standards (0 to 500 ng/mL), the assay strips became less dark. As shown in Figure 6b, the ODR values decrease rapidly with increasing concentrations of AFB1; at high concentrations (> 100 ng/mL) the ODR signal tends to reach a minimum gradually. This is due to the nature of the competitive assay and its sensitivity at lower concentrations of the analyte, while at higher concentrations, there are more free AFB1 to bind the antibodies, thus limiting the capturing of the antibody onto the surface-bound AFB1-BSA conjugates. The specificity of the assay was evaluated by analyzing an AFB1 standard (0.5 ng/mL) and other aflatoxins, AFB2, AFG1, AFG2 and AFM1 at much higher concentrations (2500 ng/mL). As shown as the inset of Figure 6(b), the ODR values of other aflatoxins were almost the same as the control (without AFB1, but containing biotin-labeled antibody). It is important to show that the ODR value shows a linear relationship with the logarithm of AFB1 concentration in the range of 0.5-250 ng/mL (Figure 6c). The regression equation can be represented by $ODR = 0.447 - 0.182 \times \log [AFB1]$, with a correlation coefficient $R^2 = 0.984$. With further optimization of other conditions such as silver enhancement time, solution composition and concentration, an even better detection limit may be possible. In Table 1, we have compared the present system with conventional instrumental analysis and immunoassay methods in terms of detection limit and dynamic response range. The lowest detection limits are typically achieved with conventional instrument-based methods and on various

matrices that require SPE clean-up, detection limits in the sub-ppb range and response ranges that vary over 1-2 orders of magnitudes were achieved.^{7,8,10,34} Although our SPAC system is not as impressive as HPLC, LC/MS and standard ELISA kits, it does cover a larger range of concentrations for quantitation with a respectable limit of detection (LOD) of 3 ± 1 ng/mL (equivalent to $\mu\text{g}/\text{kg}$, or ppb), as determined by $3S_y/m$ (where m is the slope of the fitting line shown in Figure 6c and of which the equation was provided above).³⁵ In comparison with the LFIA recently developed by Lee et al.,²⁴ which pioneered smartphone imaging of lateral flow immunoassays (LOD = 5 ppb), we were able to detect a low concentration of AFB1 in the same magnitude in standard solutions. Prior to each experiment, the pre-coated and blocked chips and other reagents were stored at 2-8 °C in dark. While the chips with immobilized coating antigen (BSA-AFB1 conjugates) are stable for up to two years, the aqueous solutions of antibodies prepared should be used within one month.³⁶

Real-world samples testing and validation

To evaluate the SPAC system for practical applications, we have tested corn samples that were spiked with 0, 5, 10, 25 ng/mL of AFB1. The amount of AFB1 determined in these corn samples were then quantified by the SPAC system, ELISA, and HPLC, of which the latter two methods typically being considered as gold standards. As shown in Figure 7(a), the concentration of AFB1 determined by the SPAC system is consistent (within the experimental uncertainty) with that determined by ELISA, and for the most part, with HPLC. At all concentrations tested, including the control (i.e., no AFB1 spiked), the determined concentrations of AFB1 (from 2 to 27 ng/mL) seem to be slightly higher than the amount used to spike the samples. This discrepancy is most likely attributed to the background calibration of the PC plates and the silver enhancement process. The agreement between the SPAC system and conventional methods (HPLC and ELISA) was further analyzed by preparing Bland-Altman plots (Supporting Information). Recovery rates for the SPAC method were 91-104% of the tested concentrations, 94-108% for ELISA, and 95-116% for HPLC.

To explore practical applications, we have tested potentially AFB1-containing corn samples, obtained by incubating fresh corn in a humid environment at room temperature for one week,

resulting in mold growth on the corn. Facilitating mold growth was necessary due to the challenges in locating positively aflatoxin-containing samples as food regulation agencies typically survey domestic and imported corn products, seizing those with aflatoxin contamination. For example, from 2011-2012, the Canadian Food Inspection Agency only found 6.6% of imported food products contained low levels of aflatoxin (not limited to the AFB1 variety) ranging from 0.1–1.5 ppb.³⁷ The moldy corn sample was extracted in the same manner as the fresh and spiked corn samples, and analyzed by both the SPAC system and ELISA; the determined concentrations of AFB1 were 8.36 ± 0.6 ng/mL and 8.62 ± 1.0 ng/mL, respectively (Figure 7a). Figure 7b shows the direct correlation between the SPAC and HPLC methods. Concentrations of AFB1 as determined by HPLC were typically lower than that from SPAC; linear regression analysis of the spiked samples yields a slope of 0.942 ± 0.05 (with an R^2 value of 0.993).

As a rapid on-site analytical tool for screen food toxins, the advantages and limitations of this smartphone-app-chip system must be considered. In comparison with ELISA, the SPAC system developed herein has the advantage of portability and cost effectiveness. A smartphone, that many people already have, and an inexpensive, reusable attachment (fabrication cost of \$2.90 that includes all components) are the only required “instruments”. Because of the device simplicity and simple assay fabrication (using a microfluidic channel plate on a plastic substrate), the cost of the analysis is significantly reduced, aided by to the high detection throughput and reduced reagent consumption. The total cost of the assay (chip and reagents) is approximately \$5.20 (Table S3), which is in the same range of cost of an uncoated 96 well ELISA microplate (\$3~10 depending on the quality and manufacture). Citing cost-effectiveness, the cost of the assay can be further minimized by limiting reagent use through reduction of microchannel size. In consideration of the assay duration (particularly the time-consuming coating antigen immobilization and blocking steps), for practical applications pre-coated and blocked chips can be made available for users. Due to the reduced the cost and difficulty of regeneration, the chips are intended for single use only.

As shown in Figure 6a, we can simultaneously test three samples and a blank while constructing a

calibration curve with 7 standards. Although the sensitivity of the SPAC method is still not as impressive as that of ELISA, for the purposes of AFB1 detection, the sensitivity is more than sufficient to detect the allowable limits outlined by the regulations on food safety in various regions, including China and the United States (20 ppb).^{4,5} These features make such an integrated smartphone-app-chip detection system an ideal tool for on-site screening before samples are brought to a centralized laboratory for further analysis. Compared to the smartphone-readable lateral flow immunoassays for AFB1 previously reported,²⁴ the SPAC system can be used to simultaneously detect multiple samples at any given time and analyze the image, immediately displaying the results to the user. Ozcan and co-workers have been actively working on the development smartphone-based analytical technologies that combines add-on hardware and custom apps for medical diagnostics.^{14-16,19,38-40} It is difficult to simply compare the SPAC system with their platforms as they focused on the detection of different target analytes; most notably they have pioneered the smartphone imaging of fluorescence from immunoassays carried out in microplate wells or glass cells, which possess different advantages of sample handling and in situ monitoring.^{33,38} In another example, Mudanyali et al. demonstrated a reader attachment for commercially available rapid tests, capable of transmittance and reflectance mode imaging, and indicates binary results of gold aggregated test strips (or semi-quantitative results based on the % of maximum and minimum saturation).⁴⁰ Specifically, the SPAC system described here is capable of reading colorimetric signals of chip-based immunoassays (enhanced with silver staining protocol, i.e., gold nanoparticle-promoted deposition of silver particles) that are suitable for quantitative and multiplex detection. In our laboratory, research efforts are continuously being made not only to optimize the performance of the app with respect to data transferring and location tracking, but also to improve the design of the chip-based immunoassays for an even broader application for on-site screening of food toxins or environmental pollutants.

Conclusions

In this study, we demonstrated a cost-effective, integrated smartphone-app-chip (SPAC) system for quantitation of AFB1 at ppb level in food products. The 3D printed optical attachment with a simple design can provide uniform illumination for an otherwise transparent, plastic assay chip, high quality images can be captured with the custom-developed Android app for data analysis and result display. An indirect competitive immunoassay of AFB1, was performed on a transparent plastic chip with the aid of a PDMS microfluidic channel plate, where both standard solutions and real-world samples were simultaneously tested. The achieved limit of detection (3 ppb and dynamic response range (0.5-250 ppb) are adequate for on-site testing of AFB1 in food products in China and North America. With further optimization it is possible to meet the requirement in Europe, where the MRL value for AFB1 is set at 2 ppb.⁴¹ Nevertheless, the direct comparison with gold standard ELISA and HPLC methods confirms the validity of the quantitation capability of the SPAC system, which promises to be a powerful analytical tool for rapid, low-cost, on-site screening of many other food toxins.

Acknowledgements

We gratefully acknowledge the financial support from the Natural Science Foundation of China (Grant No. 21575098; 21505098; 11504259); Shanxi Provincial government (“100-talents program”); Shanxi province international cooperation project (Grant No. 2015081019); Shanxi Special Programs for Platforms and Talents (201605D211033). This research was jointly supported by the Natural Sciences and Engineering Research Council (NSERC) of Canada.

Supporting Information

Additional experimental results and data analysis including dimension of the plastic microchip, HPLC data, comparison of experimental procedures of SPAC/HPLC/ELISA methods, Bland-Altman plots showing the SPAC/HPLC and SPAC/ELISA agreements, and the cost calculation for the SPAC tests (9 pages). This material is available free of charge via the Internet at <http://pubs.acs.org>.

References

- (1) Henry, S. H.; Bosch, F. X.; Troxell, T. C.; Bolger, P. M. *Science* **1999**, *286*, 2453–2454.
- (2) International Agency for Research on Cancer, 2002. IARC Monographs on the Evaluation of Carcinogenic Risk to Human. Some Traditional Medicines, Some Mycotoxins, Naphthalene and Styrene, <http://monographs.iarc.fr/ENG/Monographs/vol82> (accessed June 2017).
- (3) Armbrecht, B. H.; Shalkop, W. T.; Rollins, L. D.; Pohland, A. E.; Stoloff, L. *Nature* **1970**, *225*, 1062–1063.
- (4) China GB 2761-2011 Maximum Levels of Mycotoxins in Foods, Chemical Inspection & Regulation Service, http://www.cirs-reach.com/news/China_GB_2761-2011_Maximum_Levels_of_Mycotoxins_in_Foods.html, (accessed June 2017).
- (5) U.S. Department of Health and Human Services, Food and Drug Administration. Action Levels for Aflatoxins in Animal Feeds, <http://www.fda.gov/ICECI/ComplianceManuals/CompliancePolicyGuidanceManual/ucm074703.htm> (accessed June 2017).
- (6) Khayoon, W. S.; Saad, B.; Yan, C. B.; Hashim, N. H.; Ali, A. S. M.; Salleh, M. I.; Salleh, B. *Food Chem.* 2010, **118**, 882–886.
- (7) Nonaka, Y.; Saito, K.; Hanioka, N.; Narimatsu, S.; Kataoka, H. *J. Chromatogr. A* **2009**, *1216*, 4416–4422.
- (8) Li, P.; Zhang, Q.; Zhang, W. *Trends Anal. Chem.* **2009**, *28*, 1115–1126.
- (9) Kolosova, A. Y.; Shim, W. -B.; Yang, Z. -Y.; Eremin, S. A.; Chung, D.-H. *Anal Bioanal Chem.* **2006**, *384*, 286–294.
- (10) Liu, B.-H.; Hsu, Y.-T.; Lu, C.-C.; Yu, F.-Y. *Food Control*, 2013, **30**, 184–189.
- (11) Li, Z.; Wang, Y.; Wang, J.; Tang, Z.; Pounds, J. G.; Lin, Y. *Anal. Chem.* **2010**, *82*, 7008–7014.
- (12) Song, C.; Zhi, A.; Liu, Q.; Yang, J.; Jia, G.; Shervin, J.; Tang, L.; Hu, X.; Deng, R.; Xu, C.; Zhang, G. *Biosens. Bioelectron.* **2013**, *50*, 62–65.
- (13) Majdinasab, M.; Sheikh-Zeinoddin, M.; Soleimani-Zad, S.; Lu, P.; Zhang, Q.; Li, X.; Tang, X. *J. Chromatogr. B.* **2015**, *974*, 147–154.
- (14) Ozcan, A. *Lab Chip* **2014**, *14*, 3187–3194.
- (15) Wei, Q.; Nagi, R.; Sadeghi, K.; Feng, S.; Yan, E.; Ki, S. J.; Caire, R.; Tseng, D.; Ozcan, A. *ACS*

Nano **2014**, *8*, 1121–1129.

- (16) Zhu, H.; Sencan, I.; Wong, J.; Dimitrov, S.; Tseng, D.; Nagashima, K.; Ozcan, A. *Lab Chip* **2013**, *13*, 1282–1288.
- (17) Zangheri, M.; Cevenini, L.; Anfossi, L.; Baggiani, C.; Simoni, P.; Nardo, F. D.; Roda, A. *Biosens. Bioelectron.* **2015**, *64*, 63–68.
- (18) Petryayeva, E.; Algar, W. R. *Anal. Bioanal. Chem.* **2016**, *408*, 2913–2925.
- (19) Oncescu, V.; O'Dell, D.; Erickson, D. *Lab Chip* **2013**, *13*, 3232–3238.
- (20) Lee, S.; Oncescu, V.; Mancuso, M.; Mehta, S.; Erickson, D. *Lab Chip* **2014**, *14*, 1437–1442.
- (21) Lee, S.; O'Dell, D.; Hohenstein, J.; Colt, S.; Mehta, S.; Erickson, D. *Sci. Rep.* **2016**, *6*, 28237.
- (22) Coskun, A. F.; Wong, J.; Khodadadi, D.; Nagi, R.; Tey, A.; Ozcan, A. *Lab Chip* **2013**, *13*, 636–640.
- (23) Yu, L.; Shi, Z.; Fang, C.; Zhang, Y.; Liu, Y.; Li, C. *Biosens. Bioelectron.* **2015**, *69*, 307–315.
- (24) Lee, S.; Kim, G.; Moon, J. *Sensors* **2013**, *13*, 5109–5116.
- (25) Almutashri, A.; Agaian, S. *Proceedings of 2010 IEEE International Conference on Systems Man and Cybernetics (SMC)*, Oct. 10-13, 2010, pp 3942–3947.
- (26) Gupta, S.; Huda, S.; Kilpatrick, P. K.; Velez, O. D. *Anal. Chem.* **2007**, *79*, 3810–3820.
- (27) Li, Y.; Wang, Z.; Ou, L. M. L.; Yu, H.-Z. *Anal. Chem.* **2007**, *79*, 426–433.
- (28) Sapsford, K. E.; Taitt, C. R.; Fertig, S.; Moore, M. H.; Lassman, M. E.; Maragos, C. M.; Shriver-Lake, L. C. *Biosens. Bioelectron.* **2006**, *21*, 2298–2305.
- (29) Xia, X.; Liu, X.; Li, Y.; Ying, Y. *Biosens. Bioelectron.* **2013**, *47*, 361–367.
- (30) Zhang, L.; Li, X.; Li, Y.; Shi, X.; Yu, H.-Z. *Anal. Chem.* **2015**, *87*, 1896–1902.
- (31) Sia, S. K.; Linder, V.; Parviz, B. A.; Siegel, A.; Whitesides, G. M. *Angew. Chem., Int. Ed.* **2004**, *43*, 498–502.
- (32) Hong, J. I.; Chang, B. Y. *Lab Chip* **2014**, *14*, 1725–1732.
- (33) Meng, X.; Schultz, C. W.; Cui, C.; Li, X.; Yu, H.-Z. *Sens. Actuators, B* **2015**, *215*, 577–583.
- (34) Song, W.; Li, C.; Moezzi, B. *Rapid Commun. Mass Spectrom.* **2013**, *27*, 671–680.
- (35) Harris, D. C. *Quantitative Chemical Analysis*, 8th Ed., W. H. Freeman and Company, New York, 2010, pp. 103–105.

- (36) <https://www.labome.com/method/Antibody-Shelf-Life-How-to-Store-Antibodies.html>, accessed on June 2017.
- (37) Canadian Food Inspection Agency. <http://www.inspection.gc.ca/food/chemical-residues-microbiology/chemical-residues/2011-2012-aflatoxins/eng/1430757541452/1430757542530> (accessed June 2017).
- (38) Coskun, A. F.; Nagi, R.; Sadeghi, K.; Phillips, S.; Ozcan, A. *Lab Chip* **2013**, *13*, 4231–4238.
- (39) Berg, B.; Cortazar, B.; Tseng, D.; Ozkan, H.; Feng, S.; Wei, Q.; Chan, R. Y.-L.; Burbano, J.; Farooqui, Q.; Lewinski, M.; Di Carlo, D.; Garner, O. B.; Ozcan, A. *ACS Nano* **2015**, *9*, 7857–7866.
- (40) Mudanyali, O.; Dimitrov, S.; Sikora, U.; Padmanabhan, S.; Navruz, I.; Ozcan, A. *Lab Chip* **2012**, *12*, 2678–2686.
- (41) Commission Regulation (EC). (2006). No 1881/2006 of 19 December 2006 setting maximum levels for certain contaminants in foodstuffs.

Table 1. Comparison of the smartphone-app-chip (SPAC) system with other analytical methods for the detection of AFB1.

Method	Dynamic response range (ppb)	Detection limit (ppb)	Instrumentation	Ref.
HPLC	5-35	0.06	HPLC system	7
LC-MS	0.05-2.0	0.0024	LC-MS system	8
ELISA	0.1-10	0.05	Microplate reader	10
LFIA	5-1000	5	Smartphone/Lateral flow chip	24
SPAC	0.5-250	3	Smartphone/plastic assay chip	This study

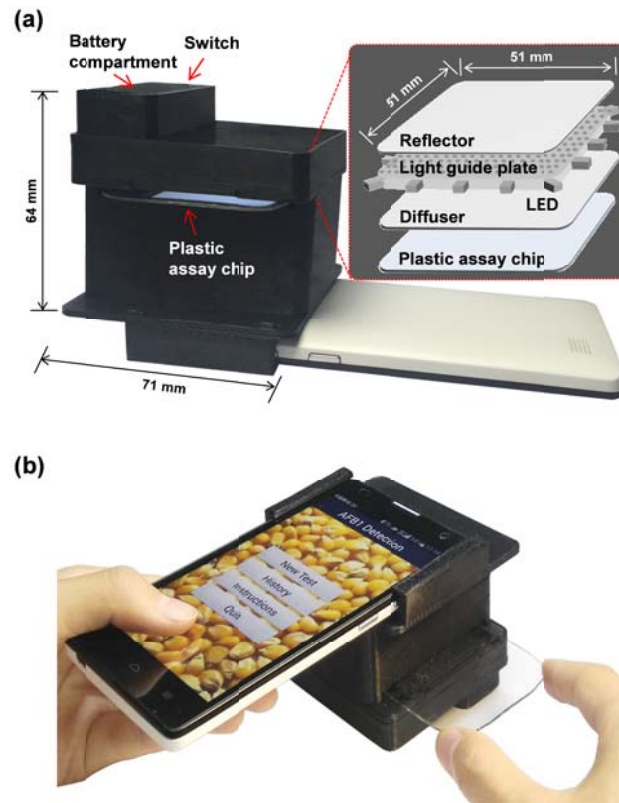


Figure 1. (a) Schematic illustration of the construction of the optical attachment for chip imaging with a smartphone. (b) The operation of chip imaging and data processing using a smartphone with the optical attachment and the custom app installed.

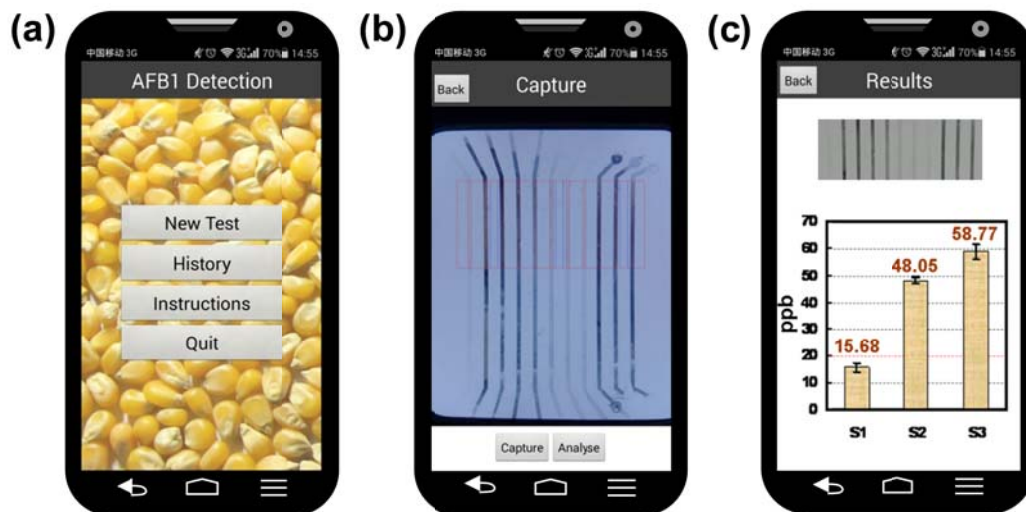


Figure 2. Screenshots of the “AFB1DET” app running on an Android smartphone. (a) Main menu with user options; (b) Preview on the screen of a plastic assay chip. The user aligns the bars of the assay with alignment aids on the screen and selects the capture function to obtain an image; (c) Results of data analysis from the captured image are displayed to the user.

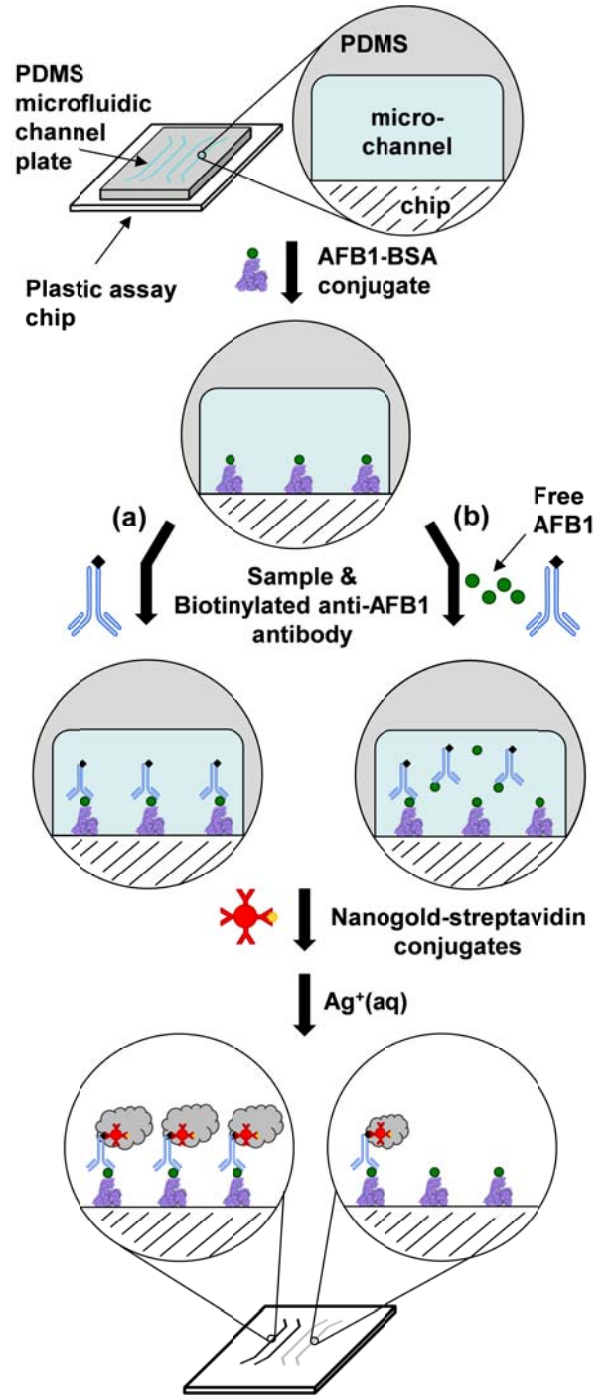


Figure 3. Schematic view of the preparation of an indirect competitive immunoassay for AFB1 with the assistance of a PDMS microfluidic channel plate on a plastic chip. In the absence of AFB1, the assay sites result in dark strips upon gold nanoparticle-promoted silver enhancement (a); in the presence of free AFB1 in the testing solution, the binding strips are less dark (b).

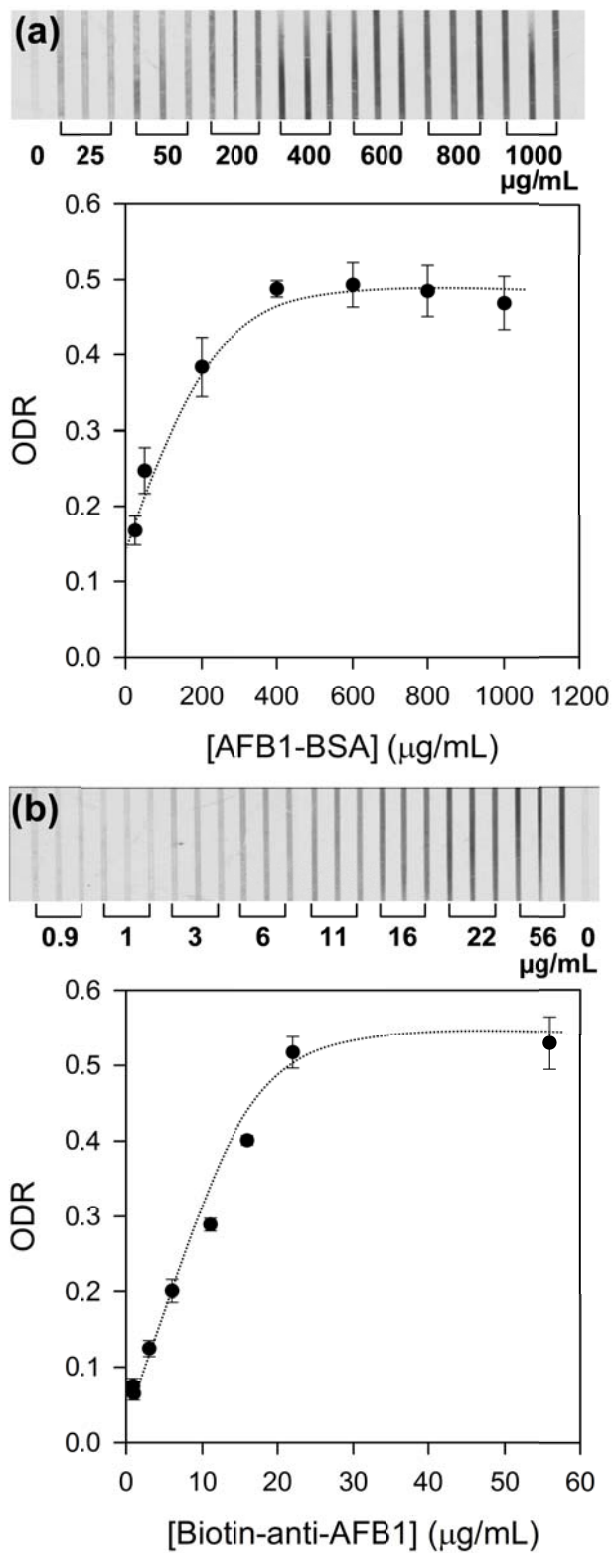


Figure 4. Optimization of the preparation conditions for the indirect competitive immunoassay of AFB1. (a) Dependence of assay signal (ODR) on the AFB1-BSA concentration; (b) The observed assay signal (ODR) as a function of the biotinylated anti-AFB1 antibody in the testing solution. The top insets are optical images of the assay chips upon silver enhancement. The dotted lines are to guide the eyes.

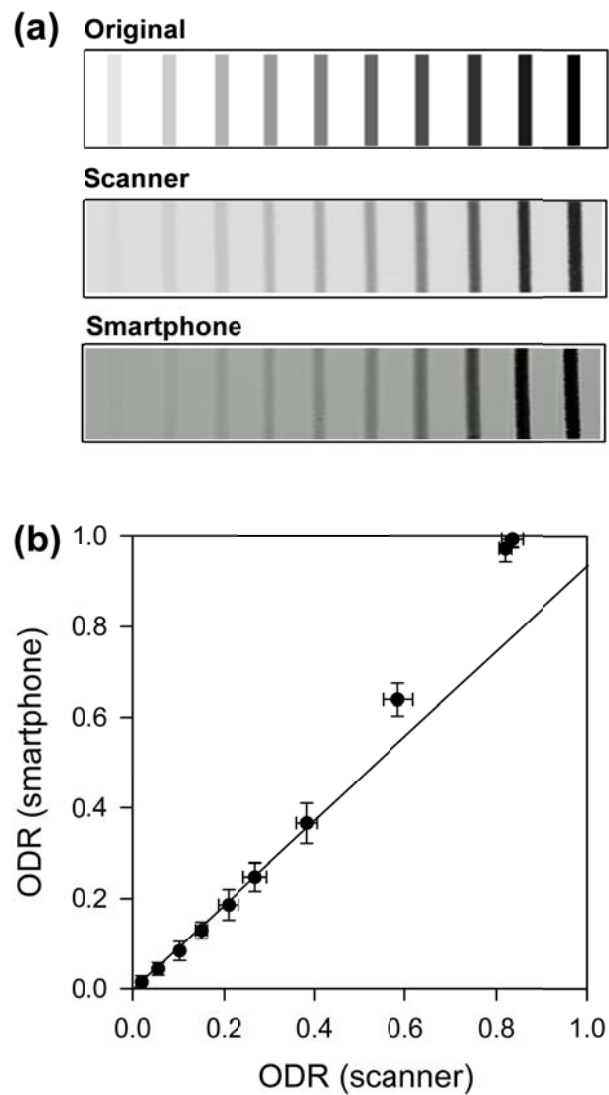


Figure 5. (a) Images obtained with a scanner and a smartphone for a set of printed ink bars with a range of grayscale values (from 0 to 255). (b) Correlation between the ODR values determined by a scanner and those by a smartphone with the optical attachment. The solid line shows the best fit to the data below an ODR value of 0.6.

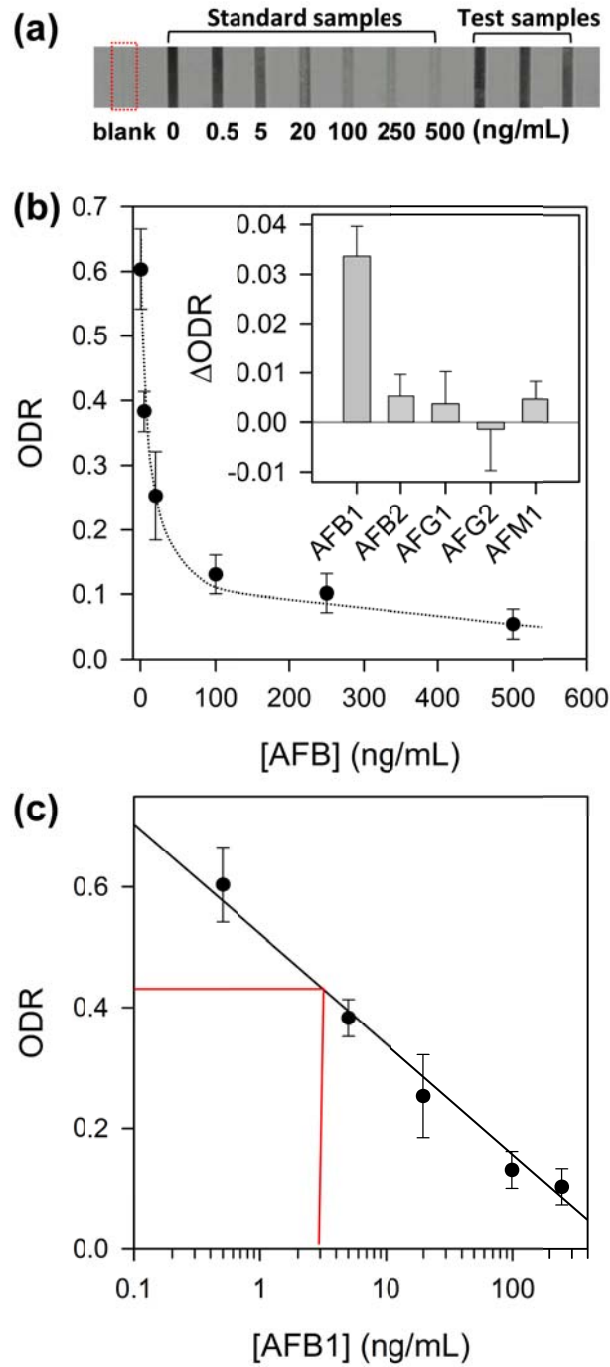


Figure 6. Quantitative detection of AFB1 in standard solutions using the SPAC system. (a) Optical image of the binding strips captured with the SPAC system. (b) Dependence of ODR signals on AFB1 concentration; the inset is the specificity test of the assay (the concentrations of AFB1 and other interfering mycotoxins are 0.5 and 2500 ng/mL, respectively). (c) Calibration curve corresponding to the AFB1 standards in the concentration range of 0.5-250 ng/mL.

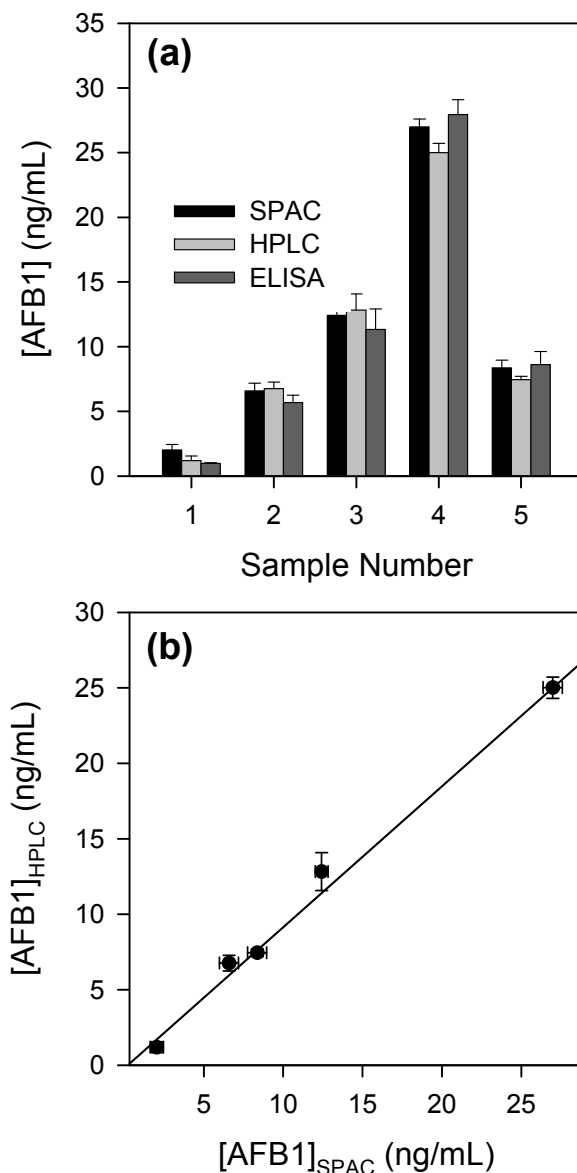


Figure 7. Comparison of the SPAC (smartphone-app-chip system) with conventional analytical methods (ELISA and HPLC) for the detection of AFB1 in corn samples. (a) Determined concentrations of AFB1 in 5 samples (samples 1-4 are spiked concentrations of 0, 5, 10, 25 ng/mL, respectively, and sample 5 is from molded corn) as measured by SPAC, HPLC, and ELISA; (b) Correlation between SPAC and HPLC results. The solid line shows the best linear fit for all five samples being tested.

TOC graphic



Supporting Information

for

Integrated Smartphone-App-Chip System for On-Site Parts-Per-Billion-Level Colorimetric Quantitation of Aflatoxins

Xiaochun Li,^{†,*} Fan Yang,[†] Jessica X. H. Wong,[‡] and Hua-Zhong Yu^{†,‡,*}

[†] *Key Laboratory of Advanced Transducers and Intelligent Control Systems (Ministry of Education and Shanxi Province), College of Physics and Optoelectronics, Taiyuan University of Technology, Taiyuan, Shanxi 030024, P.R. China*

[‡] *Department of Chemistry, Simon Fraser University, Burnaby, British Columbia V5A 1S6, Canada*

* Corresponding authors. lixiaochun@tyut.edu.cn (X.L.); hogan_yu@sfu.ca (H.-Z.Y.)

Additional experimental results and data analysis including dimension of the plastic microchip, HPLC data, comparison of experimental procedures of SPAC/HPLC/ELISA methods, Bland-Altman plots showing the SPAC/HPLC and SPAC/ELISA agreements, and the cost calculation for the SPAC tests (9 pages).

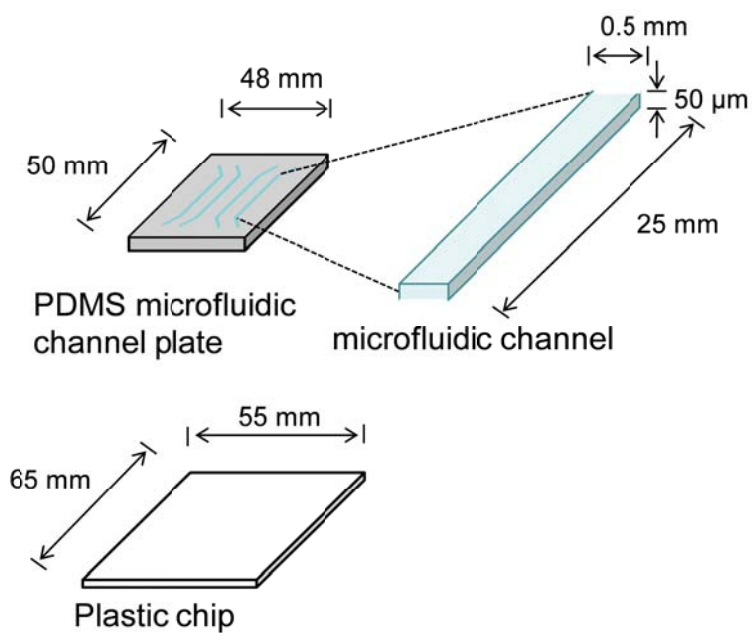


Figure S1. Physical dimensions of the PDMS microfluidic channel plate and PC plastic chip used for the SPAC assay.

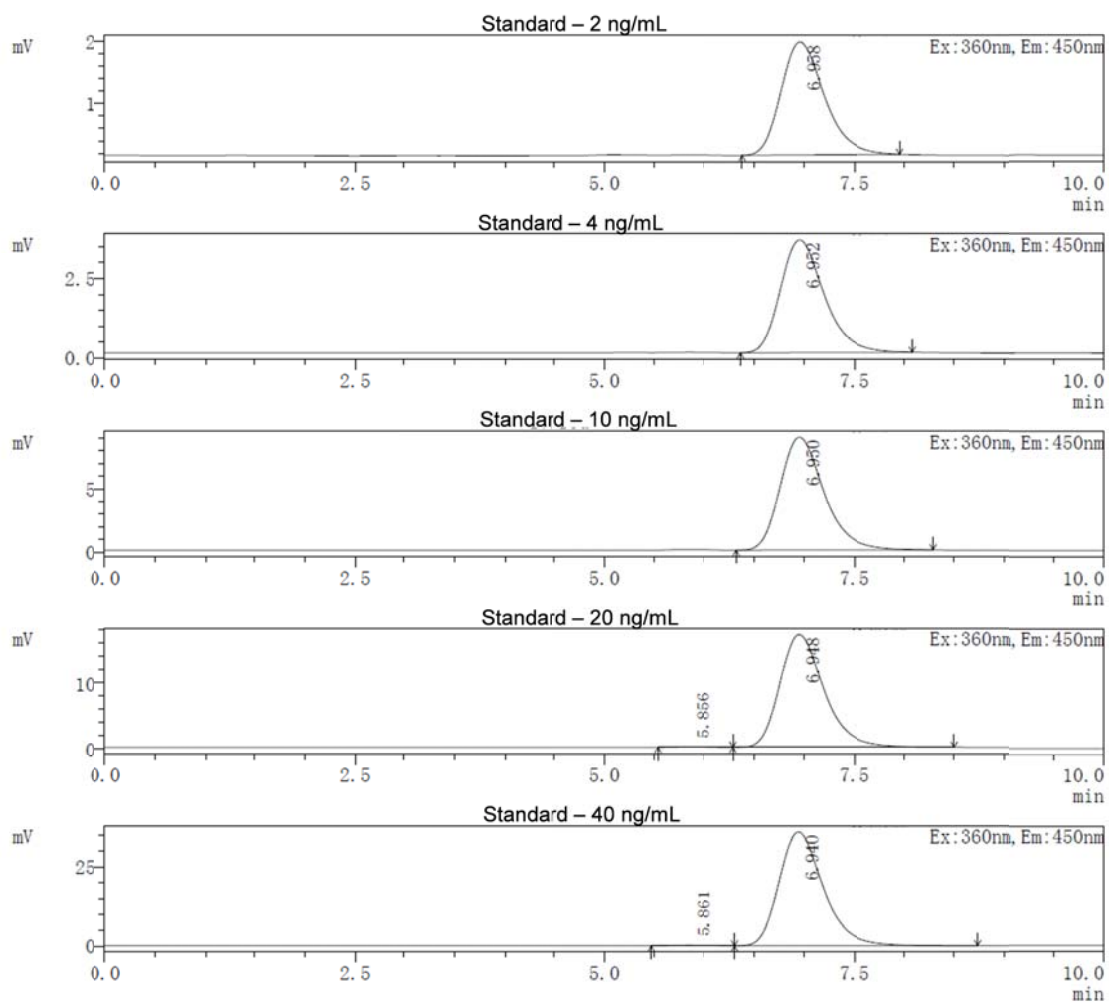


Figure S2. HPLC chromatograms of standard solutions of AFB1, prepared at 2, 4, 10, 20, and 40 ng/mL (equivalent to $\mu\text{g}/\text{kg}$, or ppb).

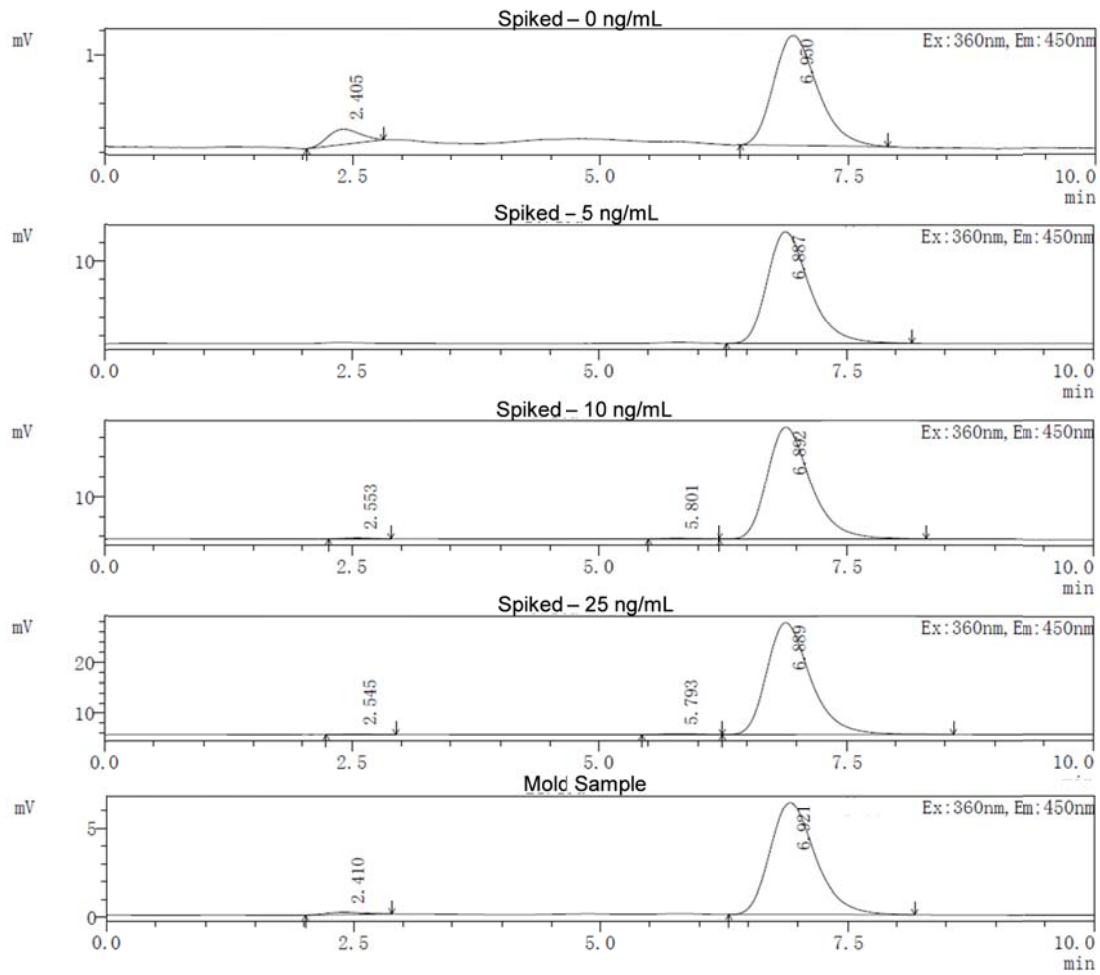


Figure S3. HPLC chromatograms of corn samples spiked with 0, 5, 10, 25 ng/mL AFB1 and a moldy corn sample.

Table S1. Summary of HPLC data for standard solutions of AFB1, corn samples spiked with AFB1 and moldy corn.

Sample (ng/mL)	Retention Time (min)	Peak Area	Concentration (ng/mL)
Std - 2	6.958	54458	2.189
Std - 4	6.952	106854	4.112
Std - 10	6.950	261920	10.071
Std - 20	6.948	521500	19.333
Std - 40	6.940	1092512	40.295
Spiked - 0	6.950	27352	1.193
Spiked - 5	6.887	179024	6.761
Spiked -10	6.892	344072	12.820
Spiked - 25	6.889	676046	25.007
Moldy corn	6.921	197856	7.453

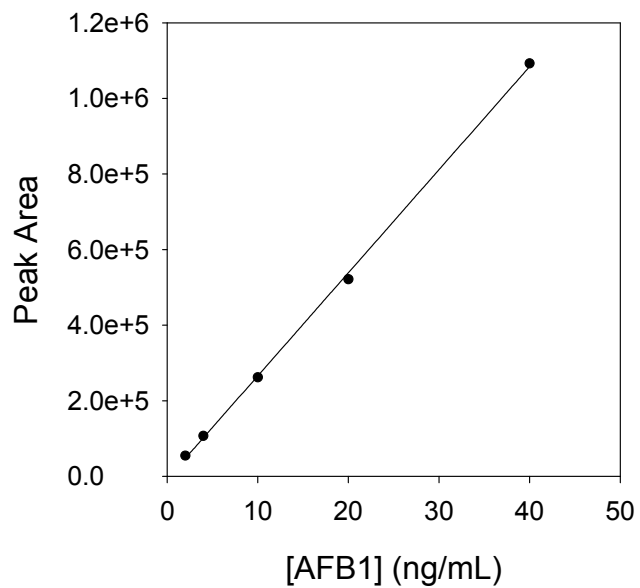


Figure S4. Calibration curve for AFB1 standard solutions (0-40 ng/mL) based on the HPLC data presented in Figure S2 and Table S1. The solid line shows the best fitting with an R^2 of 0.9994.

Table S2. Comparison of experimental procedures of the SPAC system with ELISA and HPLC methods.

Detection method		HPLC**	ELISA	SPAC
Sample preparation	Extraction	15 min	15 min	15 min
	Purification	30 min	n/a	n/a
	Derivatization	30 min	n/a	n/a
Sample detection	Chip preparation	n/a	8 h*	8 h*
	Chip blocking	n/a	3 h*	3 h*
	Sample loading/testing	30 min	30 min	30 min
	Signal enhancement	n/a	30 min	30 min
	Assay analysis	30 min	15 min	< 30 s

Note: n/a, not applicable; * these steps can be carried out prior to the tests (i.e., preloaded and blocked chips will be available for on-site testing. **HPLC does not involve the steps of chip preparation but the column needs to be preconditioned. It should be noted that the duration for each step varies significantly depending on the exact condition of the sample and instrumentation; here we just provide an estimation of the time needed for each method.

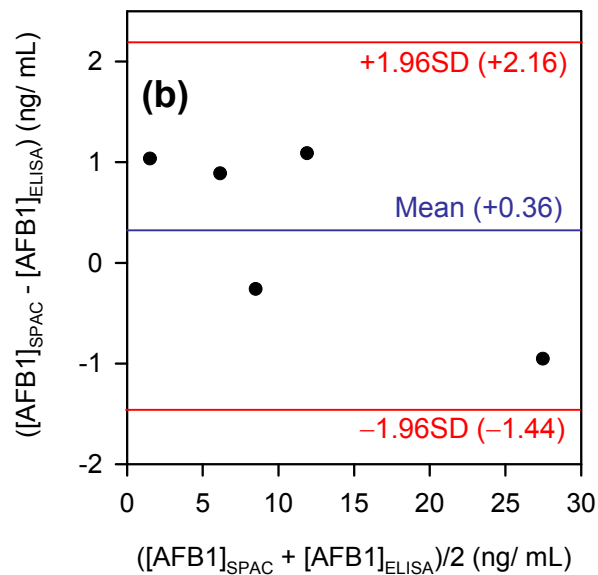
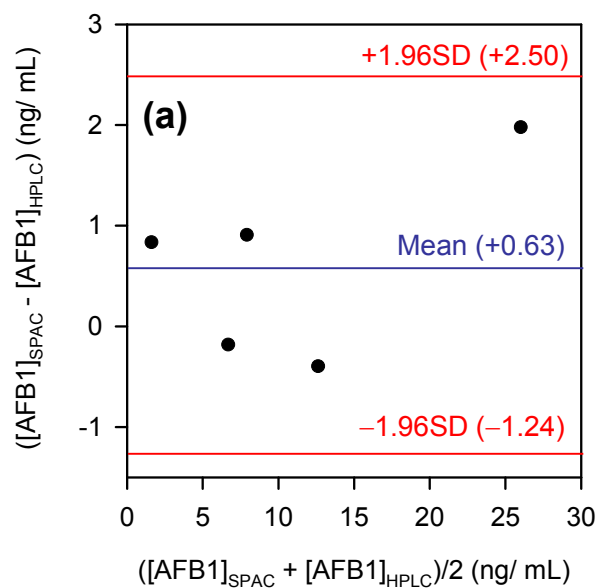


Figure S5. Bland-Altman plots showing the agreements between SPAC and HPLC (a), and between SPAC and ELISA (b), respectively. The data are based on the results presented in Figure 7(a) in the main text. For the detailed procedure to construct these plots, see Bland J. M.; Altman, D. G. Statistical methods for assessing agreement between two methods of clinical measurement, *Lancet* **1986**, 327, 307–310.

Table S3. Cost estimation of the SPAC tests.*

Chip substrate and reagent		Optical attachment	
PC plate	\$0.10	LED light source	\$0.25
AFB1(standard)	\$0.10	LGP diffuser reflector	\$1.25
Anti-AFB1 antibody	\$1.00	3D printing materials	\$1.00
AFB1-BSA (coating antigen)	\$1.30	Batteries	\$0.40
Nanogold-streptavidin conjugates	\$0.30		
Biotin labeling kit-NH2	\$0.50		
Other reagents (Buffers, NHS, EDC, etc.)	\$1.90		
Total	\$5.20	Total:	\$2.90

Note: The cost estimation listed above is in US dollars and based on multiple chips to be prepared and tested with one purchase of reagents. Taking AFB1 as an example, 5 mg AFB1-BSA was priced at ~\$ 800, and can be used for making 600 chips. Therefore, the cost of AFB1-BSA for one chip is ~\$1.30. For the PC substrate it was purchased at ~\$70 for a large panel (2.6 m²), from which about 700 chips can be made. Therefore, each of the PC substrates only costs ~\$0.10. * It should be pointed out that due to variations in the price of reagents and materials purchased from different suppliers, it is impossible to calculate the exact expense for each chip but to provide a general idea of the cost effectiveness of the SPAC tests.